

PROXIMA CENTAURI B WATER LOSS

RODRIGO LUGER

1. INTRO

We perform a suite of Markov Chain Monte Carlo (MCMC) runs to obtain constraints on the present-day water content of Proxima Centauri b using the Python code package `emcee` (Foreman-Mackey et al. 2013). MCMC allows one to sample from multi-dimensional probability distributions that are difficult or impossible to obtain directly, which is the case for the ensemble of parameters that control the evolution of the planet surface water content in `VPLANET`. In this section, we develop a framework for inferring the probability distributions of these parameters conditioned on empirical data and our understanding of the physical processes at play.

The input parameters to our model make up the state vector \mathbf{x} :

$$\mathbf{x} = \{f_{\text{sat}}, t_{\text{sat}}, \beta_{\text{xuv}}, M_{\star}, t_{\star}, a, m\}, \quad (1)$$

corresponding, respectively, to the stellar mass, the XUV saturation fraction, the XUV saturation timescale, the XUV power law exponent, the stellar age, the semi-major axis of the planet, and the mass of the planet. Given a value of \mathbf{x} , `VPLANET` computes the evolution of the system from time $t = 0$ to $t = t_{\star}$, yielding the output vector \mathbf{y} :

$$\mathbf{y}(\mathbf{x}) = \{L_{\star}, L_{\text{xuv}}, t_{\text{RG}}, m_{\text{H}}, m_{\text{H}_2\text{O}}, P_{\text{O}_2}\}, \quad (2)$$

corresponding, respectively, to the stellar luminosity, the stellar XUV luminosity, the duration of the runaway greenhouse phase, the mass of the planet’s hydrogen envelope, the mass of water remaining on its surface, and the amount of oxygen (expressed as a partial pressure) retained in either the atmosphere or the surface/mantle, all of which are evaluated at $t = t_{\star}$ (i.e., the present day). Additional parameters that control the evolution of the planet (initial water content, XUV absorption efficiency, etc.) are held fixed in individual runs; see below.

Our goal in this section is to derive posterior distributions for \mathbf{y} (and in particular for $m_{\text{H}_2\text{O}}$) given prior information on both \mathbf{x} and \mathbf{y} . Some parameters—such as the present-day stellar luminosity—are well-constrained, while others are less well-known and will thus be informed primarily by our choice of prior. This is the case for the XUV saturation fraction, saturation timescale, and power law exponent, which have been studied in detail for solar-like stars (Ribas et al. 2005) but are poorly constrained for M dwarfs. [More info on them here...](#) We therefore use flat-log priors for the saturation fraction and timescale, enforcing $-5 \leq \log(f_{\text{sat}}) \leq -2$ and $-0.3 \leq \log(t_{\text{sat}}/\text{Gyr}) \leq 1$. We use a Gaussian prior for the XUV power law exponent, with a mean of 1.23, the value derived by (Ribas et al. 2005) for solar-like stars: $\beta_{\text{xuv}} \sim \mathcal{N}(-1.23, 0.1)$. We choose an ad hoc standard deviation $\sigma = 0.1$ and verify *a posteriori* that our results are not sensitive to this choice. As we show below, β_{xuv} does not strongly correlate with the total water lost or

total amount of oxygen that builds up on the planet.

We also use a flat prior for the stellar mass ($0.1 \leq M_{\star}/M_{\oplus} \leq 0.15$). Although stronger constraints on the stellar mass exist ([cite](#)), these are derived indirectly from mass-luminosity relations; we thus enforce a prior on the present-day luminosity to constrain the value of M_{\star} via our stellar evolution model (see below). We enforce a Gaussian prior on the stellar age $t_{\star} \sim \mathcal{N}(4.8, 1.4^2)$ Gyr based on the constraints discussed in §([cite](#)).

Our prior on the semi-major axis a is a combination of a Gaussian prior on the orbital period, $P \sim \mathcal{N}(11.186, 0.002^2)$ days (Anglada-Escudé et al. 2016), and the stellar mass prior. Finally, our prior on the planet mass m combines the empirical minimum mass distribution, $m \sin i \sim \mathcal{N}(1.27, 0.18^2) M_{\oplus}$ (Anglada-Escudé et al. 2016), and the a priori inclination distribution for randomly aligned orbits, $\sin i \sim \mathcal{U}(0, 1)$, where \mathcal{U} is a uniform distribution (e.g., Luger et al. 2016).

We further condition our model on measured values of the stellar luminosity L_{\star} and stellar XUV luminosity L_{xuv} . We take $L_{\star} \sim \mathcal{N}(1.65, 0.15) \times 10^{-3} L_{\odot}$ (Demory et al. 2009) and $\log L_{\text{xuv}} \sim \mathcal{N}(-6.36, 0.3^2)$. We base the latter on Ribas et al. (2016), who compiled a comprehensive list of measurements of the emission of Proxima Centauri in the wavelength range 0.6–118 nm. Summing the fluxes over this range and neglecting the contribution of flares, we obtain an XUV flux at Proxima Centauri b $F_{\text{xuv}} \approx 252 \text{ erg cm}^{-2} \text{ s}^{-1}$, corresponding to $\log L_{\text{xuv}} = -6.36$ for $a = 0.0485 \text{ AU}$. Given the lack of uncertainties for many of the values compiled in Ribas et al. (2016) and the fact that some of those estimates are model extrapolations, it is difficult to establish a reliable error estimate for this value. We make the ad hoc but conservative choice $\sigma = 0.3$ dex, noting that the three measurements that inform the X-ray luminosity of the star in Ribas et al. (2016) (which dominates its XUV emission) have a spread corresponding to $\sigma = 0.2$ dex. However, more rigorous constraints on the XUV emission of Proxima Cen with reliable uncertainties are direly needed to obtain more reliable estimates of water loss from Proxima Cen b.

Given these constraints, we wish to find the posterior distribution of each of the parameters in Equations (1) and (2). We thus define our likelihood function \mathcal{L} for a given state vector \mathbf{x} as

$$\begin{aligned} \ln \mathcal{L}(\mathbf{x}) = & -\frac{1}{2} \left[\frac{(L_{\star}(\mathbf{x}) - L_{\star})^2}{\sigma_{L_{\star}}^2} - \frac{(L_{\text{xuv}}(\mathbf{x}) - L_{\text{xuv}})^2}{\sigma_{L_{\text{xuv}}}^2} \right] \\ & + \ln \text{Prior}(\mathbf{x}) + C, \end{aligned} \quad (3)$$

where $L_{\star}(\mathbf{x})$ and $L_{\text{xuv}}(\mathbf{x})$ are, respectively, the model predictions for the present-day stellar luminosity and stellar XUV luminosity given the state vector \mathbf{x} , L_{\star} and L_{xuv} are their respective observed values, and $\sigma_{L_{\star}}^2$ and

$\sigma_{L_{\text{xuv}}}^2$ are the uncertainties on those observations. The $\ln \text{Prior}(\mathbf{x})$ term is the prior probability and C is an arbitrary normalization constant. Expressed in this form, the observed values of L_\star and L_{xuv} are our “data,” while the constraints on the other parameters are “priors,” though the distinction is purely semantic.

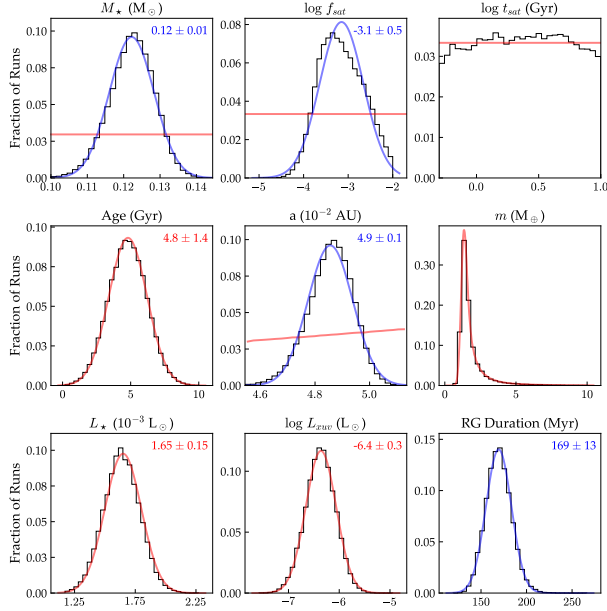


FIG. 1.— Posterior distributions for the various stellar parameters used in the model. The first eight parameters are model inputs, with their corresponding priors shown in red. The combination of these priors and the physical models in VPLANET constrain the stellar and planetary parameters shown in this section. Blue curves show Gaussian fits to the posterior distributions, with the mean and standard deviation indicated at the top right. The last panel shows the duration of the runaway greenhouse phase for Proxima Centauri b, one of the model outputs, which we find to be 169 ± 13 Myr.

Given this likelihood function, we use MCMC to obtain the posterior probability distributions for each of the parameters of interest. We draw each of the \mathbf{x} from their respective prior distributions and run 40 parallel chains of 5,000 steps each, discarding the first 500 steps as burn-in. The marginalized posterior distributions for the stellar mass, saturation fraction, saturation timescale, age, semi-major axis, planet mass, present-day stellar luminosity, present-day stellar XUV luminosity, and duration of the runaway greenhouse are shown in Figure 1 as the black histograms. The red curves indicate our priors/data, and the purple curve is a Gaussian fit to the runaway greenhouse duration posterior, yielding $t_{\text{RG}} = 169 \pm 13$ Myr.

By construction, the planet mass, stellar age, present-day stellar luminosity, and present-day stellar XUV luminosity posteriors reflect their prior distributions. As mentioned above, the stellar mass posterior is entirely informed by the luminosity posterior via the Spada et al. (2013) stellar evolution tracks. The stellar mass in turn constrains the semi-major axis (via the prior on the period and Kepler’s laws). The XUV saturation fraction is fairly well constrained by the present-day XUV luminosity; a log-normal fit to its posterior yields $\log f_{\text{sat}} =$

-3.1 ± 0.5 , which is fully consistent with the observation that M dwarfs saturate at or below $\log f_{\text{sat}} \approx -3$ (cite). The longer tail at high f_{sat} results from the fact that this parameter is strongly correlated with the saturation timescale, t_{sat} (see Figure 5 below). If saturation is short-lived, the initial saturation fraction must be higher to match the present-day XUV luminosity. Interestingly, our runs do not provide any constraints on t_{sat} , whose value is equally likely (in log space) across the range $[0.5, 10]$ Gyr. Finally, the posterior for the XUV power law exponent β_{xuv} (not shown in the Figure) is the same as the adopted prior, as the present data is insufficient to constrain it.

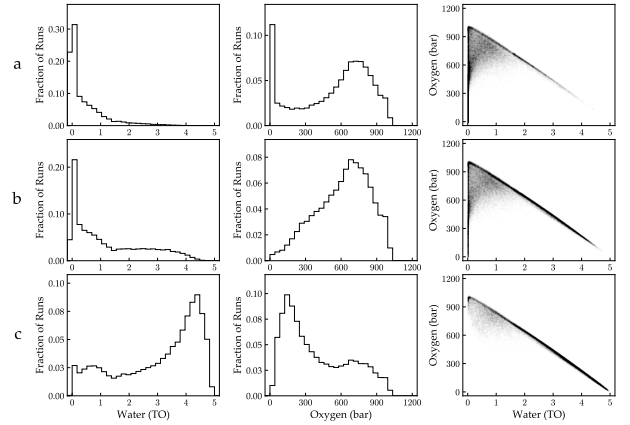


FIG. 2.— Marginalized posteriors for the present-day water content (left) and atmospheric oxygen pressure (center) on Proxima Cen b. The joint posteriors for these two parameters are shown at the right. (a) Posteriors for the default run ($m_{\text{H}_2\text{O}}^0 = 5$ TO, $m_{\text{H}}^0 = 0$, $\epsilon_{\text{xuv}} = 0.15$, $\zeta_{\text{O}_2} = 0$). (b) Same as (a), but for $\epsilon_{\text{xuv}} = 0.05$. (c) Same as (a), but for $\epsilon_{\text{xuv}} = 0.01$. For $\epsilon_{\text{xuv}} \gtrsim 0.05$, the planet loses close to 5 TO of water and builds up between 500 and 900 bars of O_2 in most runs. For $\epsilon_{\text{xuv}} \sim 0.01$, the planet loses less water and builds up less O_2 , though the loss of more than 1 TO is still likely.

The two quantities that are of the most interest to us — the final water content $m_{\text{H}_2\text{O}}$ and final O_2 atmospheric pressure P_{O_2} of Proxima Cen b — depend on four additional parameters we must specify: the initial water content $m_{\text{H}_2\text{O}}^0$, the initial hydrogen mass m_{H}^0 (if the planet formed with a primordial envelope), the XUV escape efficiency ϵ_{xuv} , and the O_2 uptake efficiency ζ_{O_2} of the planet surface. In principle, planet formation models could provide priors on $m_{\text{H}_2\text{O}}^0$ and m_{H}^0 , but such models depend on additional parameters that are unknown or poorly constrained. The same is true for the XUV escape efficiency, which can be modeled as in Ribas et al. (2016), and the rate of absorption of O_2 at the surface, which can be computed as in Schaefer et al. (2016). However, given the large number of unknown parameters needed to constrain these four parameters, for simplicity we perform independent MCMC runs for fixed combinations of these. By doing this, we circumvent potential biases arising from incorrect priors on these parameters while still highlighting how our results scale for different assumptions about their values.

In the runs discussed below, our default values are $m_{\text{H}_2\text{O}}^0 = 5$ TO, $m_{\text{H}}^0 = 0$ M_{\oplus} , $\epsilon_{\text{xuv}} = 0.15$, and $\zeta_{\text{O}_2} = 0$,

and we vary each of these parameters in turn. Figure 2 shows the marginalized posterior distributions for the present-day water content (left column) and present-day O_2 atmospheric pressure (middle column), as well as a joint posterior for the two parameters (right column) for three different values of ϵ_{XUV} : **(a)** 0.15, **(b)** 0.05, and **(c)** 0.01. In the first two cases, the planet loses all or nearly all of the 5 TO it formed with, building up several hundred bars of O_2 (with distributions peaking at about 700 bars and with a spread of several hundred bars). For $\epsilon_{\text{XUV}} = 0.15$, about 10% of runs result in no substantial oxygen remaining in the atmosphere; in these runs, the escape was so efficient as to remove all of the O_2 along with the escaping H . In the final case, the amount of water lost is significantly smaller: about 2 TO on average, with a peak in the distribution corresponding to a loss of about 0.8 TO. The amount of O_2 remaining is similarly smaller, but still exceeding 100 bars and with similar spread as before. Finally, the joint posterior plots emphasize how correlated the present-day water and oxygen content of Proxima Cen b are. Since the rate at which oxygen builds up in the atmosphere is initially constant at first (?), and since the amount of water lost scales with the duration of the escape period, there is a tight linear correlation between the two quantities (lower right hand corner of the joint posterior plots). However, as the atmospheric mixing ratio of oxygen increases, the rate at which hydrogen escapes—and thus the rate at which oxygen is produced—begins to decrease, leading to a break in the linear relationship once ~ 600 –700 bars of oxygen build up and leading to the peak in the O_2 posteriors at around that value.

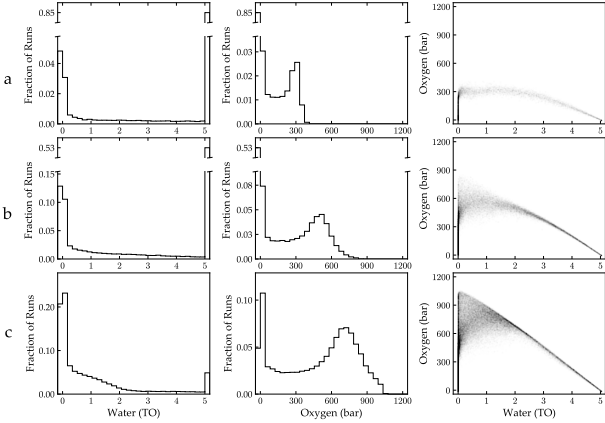


FIG. 3.— Similar to Figure 2, but this time varying the initial mass of the primordial hydrogen envelope of Proxima Cen b. Other parameters are set to their default values. The initial mass of hydrogen is $m_H^0 =$ **(a)** $0.01 M_\oplus$, **(a)** $0.001 M_\oplus$, and **(a)** $0.0001 M_\oplus$. Note the broken axes in the first two rows. In the first two cases, no water is lost in more than half of the runs; in such cases, a thin hydrogen envelope remains today. In the final case, most planets lost all their hydrogen and all their water. In order to prevent the runaway loss of its water, Proxima Cen b must have formed with more than 0.01% of its mass in the form of a hydrogen envelope.

In Figure 4 we explore the effect of varying the initial hydrogen content of the planet.

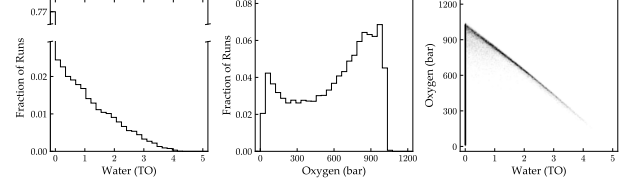


FIG. 4.— Planet posteriors (magma).

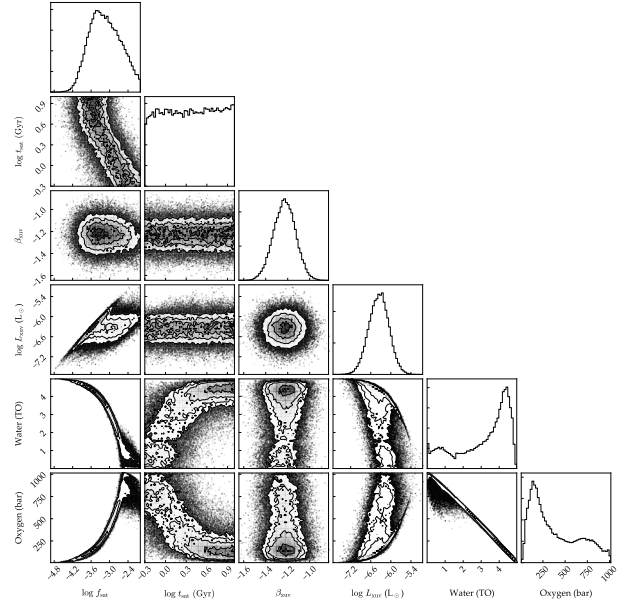


FIG. 5.— Correlations. Beta isn't correlated with water because it's too late to matter.

REFERENCES

- Anglada-Escudé, G., Amado, P. J., Barnes, J., Berdiñas, Z. M., Butler, R. P., Coleman, G. A. L., de La Cueva, I., Dreizler, S., Endl, M., Giesers, B., Jeffers, S. V., Jenkins, J. S., Jones, H. R. A., Kiraga, M., Kürster, M., López-González, M. J., Marvin, C. J., Morales, N., Morin, J., Nelson, R. P., Ortiz, J. L., Ofir, A., Paardekooper, S.-J., Reiners, A., Rodríguez, E., Rodríguez-López, C., Sarmiento, L. F., Strachan, J. P., Tsapras, Y., Tuomi, M., & Zechmeister, M. 2016, *Nature*, 536, 437
- Demory, B.-O., Ségransan, D., Forveille, T., Queloz, D., Beuzit, J.-L., Delfosse, X., di Folco, E., Kervella, P., Le Bouquin, J.-B., Perrier, C., Benisty, M., Duvert, G., Hofmann, K.-H., Lopez, B., & Petrov, R. 2009, *A&A*, 505, 205
- Foreman-Mackey, D., Hogg, D. W., Lang, D., & Goodman, J. 2013, *PASP*, 125, 306
- Luger, R., Lustig-Yaeger, J., Fleming, D. P., Tilley, M. A., Agol, E., Meadows, V. S., Deitrick, R., & Barnes, R. 2016, *ArXiv e-prints*
- Ribas, I., Bolmont, E., Selsis, F., Reiners, A., Leconte, J., Raymond, S. N., Engle, S. G., Guinan, E. F., Morin, J., Turbet, M., Forget, F., & Anglada-Escudé, G. 2016, *A&A*, 596, A111
- Ribas, I., Guinan, E. F., Güdel, M., & Audard, M. 2005, *Astrophys. J.*, 622, 680
- Schaefer, L., Wordsworth, R. D., Berta-Thompson, Z., & Sasselov, D. 2016, *ApJ*, 829, 63
- Spada, F., Demarque, P., Kim, Y.-C., & Sills, A. 2013, *ApJ*, 776, 87